Separation Science and Technology
Publication details, including instructions for authors and subscription information:
http://www.informaworld.com/smpp/title~content=t713708471

CFD analysis on fluid flow through multifilament woven filter cloths

Kuo-Lun Tung[a]; Jia-Shyan Shiau[a]; Ching-Jung Chuang[a]; Yu-Ling Li[a]; Wei-Ming Lu[b]
[a] Department of Chemical Engineering, Chung Yuan University, Taoyuan, Taiwan, ROC [b] Department of Chemical Engineering, National Taiwan University, Taipei, Taiwan, ROC

Online publication date: 23 April 2002

To cite this Article Tung, Kuo-Lun , Shiau, Jia-Shyan , Chuang, Ching-Jung , Li, Yu-Ling and Lu, Wei-Ming(2002) 'CFD analysis on fluid flow through multifilament woven filter cloths', Separation Science and Technology, 37: 4, 799 — 821
To link to this Article: DOI: 10.1081/SS-120002218
URL: http://dx.doi.org/10.1081/SS-120002218

SEPARATION SCIENCE AND TECHNOLOGY, 37(4), 799–821 (2002)

CFD ANALYSIS ON FLUID FLOW THROUGH MULTIFILAMENT WOVEN FILTER CLOTHS

Kuo-Lun Tung,[1,*] Jia-Shyan Shiau,[1] Ching-Jung Chuang,[1] Yu-Ling Li,[1] and Wei-Ming Lu[2]

[1]Department of Chemical Engineering, Chung Yuan University, Chungli, Taoyuan 320, Taiwan, ROC
[2]Department of Chemical Engineering, National Taiwan University, Taipei 106, Taiwan, ROC

ABSTRACT

The effects of woven structures on fluid flow through the basic weaves of multifilament woven filter cloths were studied numerically by using the fluid-flow software FLUENT™. From results of the numerical solution, the flow pattern and the resistance to flow in the interstices were obtained. Results of this work show that the construction of the fabric pores has a significant influence on the flow pattern in the interstices and the downstream. It is also shown that the plain weave gives the highest fluid-flow resistance while the satin weave gives the lowest under the same thread count. Furthermore, in the case of tightly woven filter cloths, the flow is predominantly through the yarns of the cloth; while the flow will generally be directed around the yarns of a loosely woven cloth, especially if the yarns are

*Corresponding author. Fax: (886) 3-4372159; E-mail: kuolun@cycu.edu.tw

twisted tightly. A comparison of fluid flow through multifilament woven filter cloth with that of monofilament woven filter cloth is also discussed.

Key Words: Filter cloth; Multifilament; Flow pattern; Resistance to flow

INTRODUCTION

Woven filter cloths play a vital role in numerous industrial solid–liquid separation processes. In view of such a complicated geometry of the various woven patterns of the filter cloth, shown in Fig. 1, it is crucial to examine the effect of woven patterns and fabric yarn forms on the hydrodynamic behavior of

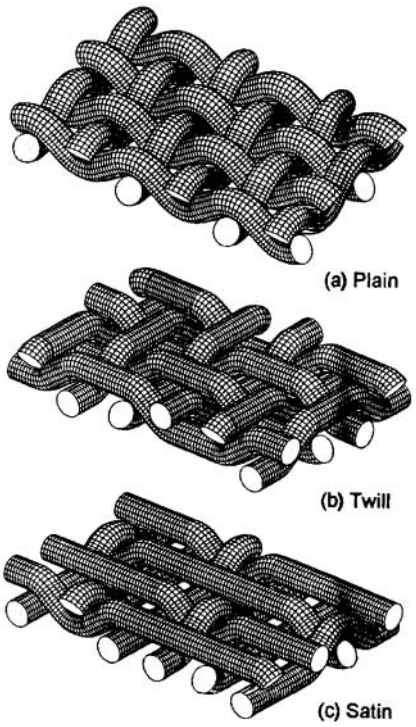

Figure 1. Three basic weave models of woven filter cloths. "▦" denotes interfiber region in multifilament fabrics.

MARCEL DEKKER, INC.
270 Madison Avenue, New York, New York 10016

fluid flow through woven fabrics in order to investigate the effect of the woven structure on the flow pattern, flow resistance, filtrate clarity, and fouling phenomena in fabric pores.

Previous investigations of fluid flow through woven fabrics and fabriclike structures assumed diverse forms, with various forms of fabric yarn in view. For monofilament fabric yarn, many researchers have approached the problem by comparing the flow situation in the woven fabric (1) to: (i) an assembly of orifices (2–4), (ii) a random packed bed, and (iii) an extension of the available analytical solutions for creeping flow over cylinders (5). It had been shown that analysis based on orifice flow is most successful in correlating experimental results of monofilament woven filter fabrics (1). However, examination of experimental data indicates serious discrepancies in the predicted and practical values for multifilament woven filter cloths. Failure occurs when flow can take place through and around the yarns making up the cloths. In multifilament yarns composed of continuous or staple fibers, the number of fibers per yarn and their twist will decide the permeability and the division of flow through and around the yarns. For instance, Robertson (4) plotted the experimental values of $\log C_D$ against $\log Re$ for air flow through plain weave metallic meshes and obtained a good correlation between these two dimensionless variables based on the orifice model proposed by Backer (6). However, the technique failed when it was applied to loosely woven multifilament cloths of different weave patterns. Backer (6) suggested that this failure was due to the fact that the fabric pores of a multifilament cloth are too complicated to be characterized by the simple projected open area used in Robertson's correlation. Backer considered that the factor governing the flow rate to the greatest extent was the minimum pore cross-sectional area, and showed that use of a minimum pore area reduced greatly the scatter produced by calculations based on the projected open area. In another extreme case, some of the cloths were woven so tightly as to prevent flow around the yarns, and thus also resulted in a failure of orifice model (7). For multifilament woven filter cloths, the flow division depends mainly on the size and distribution of the interyarn and interfiber pores. McGregor (8) used an analytical solution of the Navier–Stokes equations for flow through an assembly of spheres in predicting the division of flow between intrayarn and interyarn zones. Van den Brekel and de Jong (9) also proposed a simplified model to predict fabric permeability theoretically. In their theoretical model, the interyarn and interfiber were considered parallel regions; a local porosity model has been proposed according to the Kozeny equation. They concluded that when fluid flows through a fabric, the major part of the liquid will pass through the interfiber region; and their proposed model was suitable only for tightly woven multifilament fabrics. Rushton (10) claimed that in order to describe the specific permeability of a fabric textile, it is necessary to consider the division of fluid flow through and around the yarns of the filter cloth. In the case of tightly woven filter cloths, the flow is

predominant through the yarns of the cloth and it is possible to correlate flow data in terms of the diameter of the fibers in the yarn. On the other hand, however, the flow will be directed generally around the yarns of a loosely woven cloth, especially if the yarns are twisted tightly, and the yarn diameter will become more important. Many practical cases of cloths woven from multifilament yarns fall between these two extremes. From the previous review, one can know that most of the available results take into account the general fluid flow far from the filter media, and they are mainly concerned only with the pressure drop problem without any information about the microscopic details of velocity profile and pressure contour in the interstices. Recently, Lu et al. (11) calculated the velocity profile and pressure contour in the interstices of monofilament filter cloth successfully. Computational fluid dynamic (CFD) techniques provide a direct route from the microscopic detail of velocity profile and pressure contour in the interstices to the macroscopic property of experimental interest as the pressure drop across the interstices. It is difficult or almost impossible to carry out experiments in an extremely small interstice, say 10 μm, while a CFD technique would be perfectly feasible.

In this work, the flow of fluid through the three basic weaves of modeled multifilament filter cloth is studied numerically by using the fluid-flow software FLUENT. The results obtained by such an approach can give better understanding of the flow pattern in the woven fabric pore and prove useful in examining the initial stage of cake filtration as well as the effect of weaves on fouling phenomenon within a filter cloth. A comparison of fluid flow through multifilament woven filter cloth with that of monofilament woven filter cloth is also discussed.

THEORETICAL MODELING

Models of Multifilament Woven Filter Cloths

For woven filter cloths, the crossing of yarns during weaving produces various textures. The basic structures of the most common weaves are shown in Fig. 1; they are (a) plain weave, (b) twill weave, and (c) satin weave. The basic structures of these three most common weaves of filter cloths are a combination of the four basic pore models, as shown in Fig. 2 (6). Each type of pore is constructed with four fabric yarns. Figure 3 shows three widely used types of yarn, these being monofilament, multifilament, and spun staple. Monofilament is a single continuous filament, while multifilament is a bundle of identical continuous filaments. Thus, although multifilament is produced in much the same way as the monofilament, the multifilament has a multiplicity of much finer holes. Spun staple yarn manufactured from short fibers using spinning techniques

MARCEL DEKKER, INC.
270 Madison Avenue, New York, New York 10016

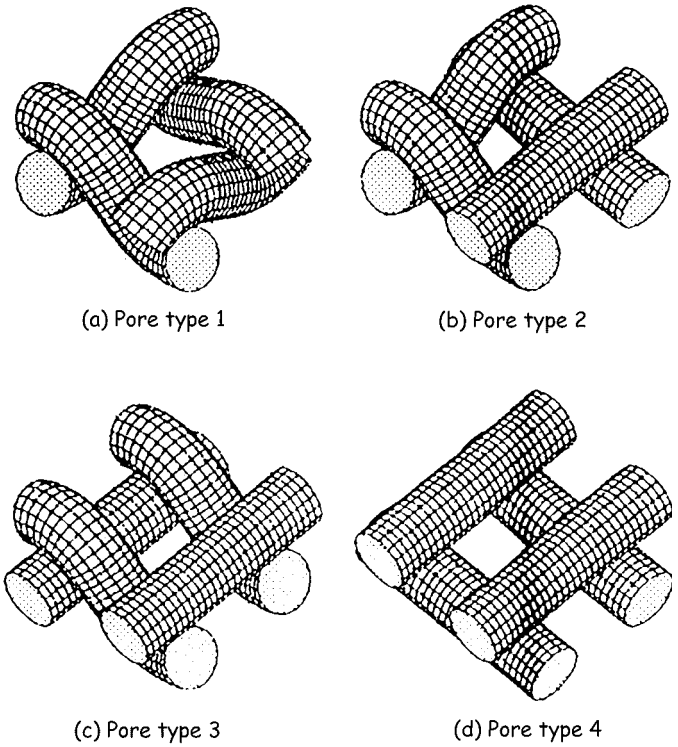

Figure 2. Four types of basic woven fabric pore models. "▦" denotes interfiber region in multifilament fabrics.

developed considerably longer and more crimped fibers of wool. The physical differences between these three types of yarn have a significant effect on the filtration characteristics of cloths woven from them. In view of the complicated geometry of the various woven patterns of filter cloth and types of fabric yarn, the main difficulty encountered when dealing with the flow of fluid through woven filter cloth is the highly tortuous geometry of the fibers and yarns that make up the cloth. In a recent article by the authors (9), the effect of pore construction on the flow field and pressure drop of the fluid flow through these four basic monofilament fabric pores had been studied numerically by using the commercially available software FLUENT. In this study, emphasis will be focused on the effect of types of fabric yarn on the performance of woven filter cloths, especially for multifilament yarns. Before the calculation, the hydraulic radius and porosity of a woven filter medium should be defined in advance. The crimp diagrams of pore type 1 are shown in Fig. 4. To estimate the hydraulic

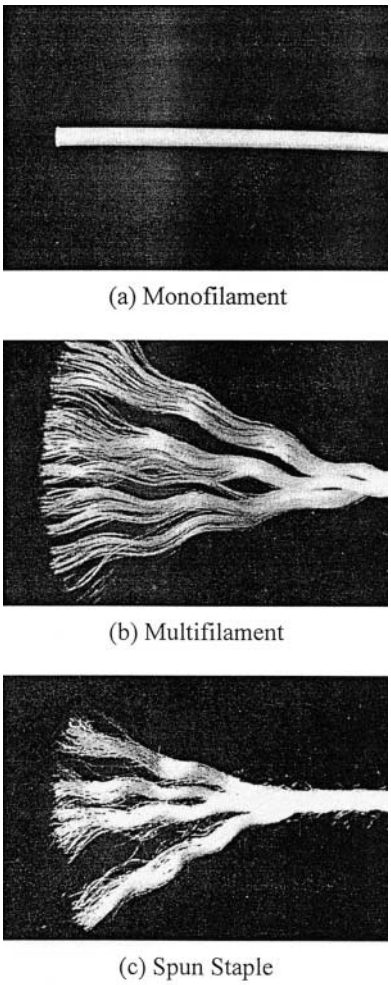

Figure 3. Three types of yarn forms: (a) monofilament, (b) multifilament, and (c) spun staple (Scapa Filtration Co.).

radius and porosity of a woven filter medium, it is assumed that the fabric yarn is made of cylindrical yarn with diameter d_w in the warp direction and d_f in the weft direction. The radius of the torus is equal to the arithmetic mean of the warp and weft (filling) yarn diameters, and the greek letter α denotes the angle of inclination of the yarn system at the central plane of the fabric. The yarn spacings in the warp and weft directions are assumed to be l_w and l_f, respectively. For a three-dimensional (3D) flow channel, the hydraulic radius r_H is defined with the

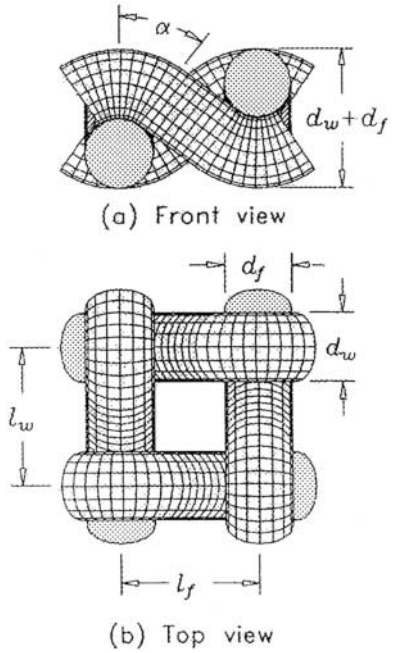

Figure 4. Crimp diagram of fabric pore type 1. "▦" denotes interfiber region in multifilament fabrics.

volume of the void and the wetted surface of the unit pore model as follows:

$$r_{\mathrm{H}} = \frac{\text{volume of void}}{\text{wetted surface}} \tag{1}$$

Using the same definition and assuming that the yarn diameters and yarn spacings are equal to d and l, respectively, both in the warp and weft directions, the equivalent pore diameter D_{e} and the porosity ϵ for type 1 pore can be obtained as follows:

$$D_{\mathrm{e}} = 4r_{\mathrm{H}} = \frac{4l^2 - \pi d(\sqrt{l^2 - 3d^2} + 2\alpha d)}{\pi(\sqrt{l^2 - 3d^2} + 2\alpha d)} \tag{2}$$

and

$$\epsilon = 1 - \frac{\pi d(\sqrt{l^2 - 3d^2} + 2\alpha d)}{4l^2} \tag{3}$$

MARCEL DEKKER, INC.
270 Madison Avenue, New York, New York 10016

Details of the derivations of these equations are presented in our previous work (12). Furthermore, fabric constructions have two or three types of basic unit pores, which are shown in Fig. 2. As shown in Fig. 1(a) and (b), the plain and 2/2 twill weaves consist entirely of type 1 pores (plain pores) and type 2 pores (twill pores), respectively. The 4/1 satin, however, always contains a fifth part of type 4 pores and four parts of type 2 pores, independent of their position on the fabric. Thus, under the same driving pressure, the approaching velocity, equivalent diameter, effective fraction open area, and orifice perimeter of satin weaves may be characterized by weighting the contribution of type 2 and type 4 pores as follows:

$$U_\infty = \frac{4}{5}U_{\infty(2)} + \frac{1}{5}U_{\infty(4)} \tag{4a}$$

$$D_e = \frac{4}{5}D_{e(2)} + \frac{1}{5}D_{e(4)} \tag{4b}$$

$$\alpha_p = \frac{4}{5}\alpha_{p(2)} + \frac{1}{5}\alpha_{p(4)} \tag{4c}$$

$$W_p = \frac{4}{5}W_{p(2)} + \frac{1}{5}W_{p(4)} \tag{4d}$$

In order to calculate the flow field and flow resistance of fluid flow through the multifilament fabric pore, the governing equations and boundary conditions and the numerical method are defined in the next two sections, respectively, based on the proposed models.

Governing Equations

The flow field can be obtained by solving the equation of continuity and the momentum balance equations of the system with appropriate boundary conditions. The major assumptions of this modeling approach are:

1. the flow of fluid in the domain of this study is assumed to be laminar, steady state, and isothermal;
2. the upstream and downstream velocity profiles far from the inlet and outlet of the filter pore model are uniform; and
3. the fabric yarn is regarded as a permeable object with a unidirectional permeability. The homogeneous permeability, K_y, of fabric yarn is defined to represent the tightness of fabric yarn.

MARCEL DEKKER, INC.
270 Madison Avenue, New York, New York 10016

The dimensionless equation of continuity and equation of motion for the system are as follows:

(I) Equation of continuity

$$\nabla v^* = 0 \tag{5}$$

(II) Momentum equation

$$v^* \nabla v^* = -\nabla P^* + \frac{1}{Re}\nabla^2 v^* + \frac{1}{Fr} g^* \tag{6}$$

All space variables and flow quantities are normalized with respect to the equivalent pore diameter, D_e, and approach velocity, U_∞, far from the inlet of the filter pore.

The boundary conditions for Eqs. (3) and (4a)–(d) are as follows, and the system is shown in Fig. 5.

(I) Upstream inlet and downstream outlet: the upstream and downstream velocity profiles far from the inlet and outlet of the filter pore model are uniform. Both the inlet and outlet of the calculation domain are set to $5(l - d)$ from the filter pore model:

$$v_z^* = v_z/u_\infty = 1, \quad v_x^* = v_y^* = 0 \tag{7}$$

(II) Symmetric y–z plane 3:

$$\frac{\partial v_z^*}{\partial x^*} = 0, \quad v_x^* = 0 \tag{8}$$

(III) Symmetric x–z plane 4:

$$\frac{\partial v_z^*}{\partial y^*} = 0, \quad v_y^* = 0 \tag{9}$$

(IV) Fabric surface:

Since the fabric is regarded as a permeable object, the fabric surface is a porous wall and its boundary condition can be expressed as:

$$\nabla P^* = -\frac{D_e^2}{K_y \mathrm{Re}} v^* \tag{10}$$

Numerical Method

A commercial CFD software package FLUENT (Version 4.5) was used to calculate the flow field in the filter pore. About 12,000 ($17 \times 17 \times 37$)

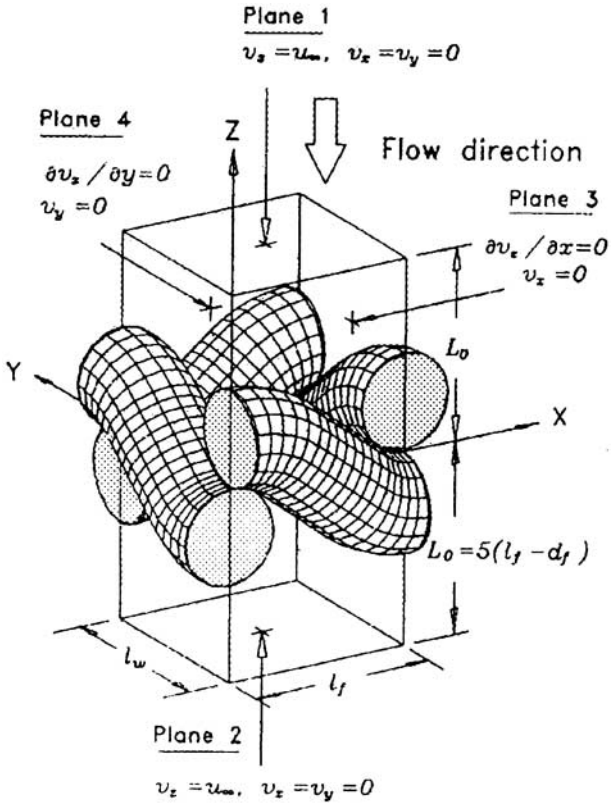

Figure 5. A schematic diagram for calculating domain and boundary conditions. "▦" denotes interfiber region in multifilament fabrics.

cells were used in the numerical computation. Figure 6 shows the top-sectional views of the meshes for calculation in the $x-y$ plane. Successive slices of the four different fabric pores were taken at levels of $d/8$. The SIMPLE algorithm (12) with the power-law difference scheme and single direction sweep solution method were used in this study. The method basically involves dividing the calculation domain into a number of nonoverlapping control volumes, each containing a cell node at its center. Then the differential equations of interest are integrated over each control volume assuming a power-law function profile for variation of the dependent variable between adjacent grids for evaluation of integrals. The

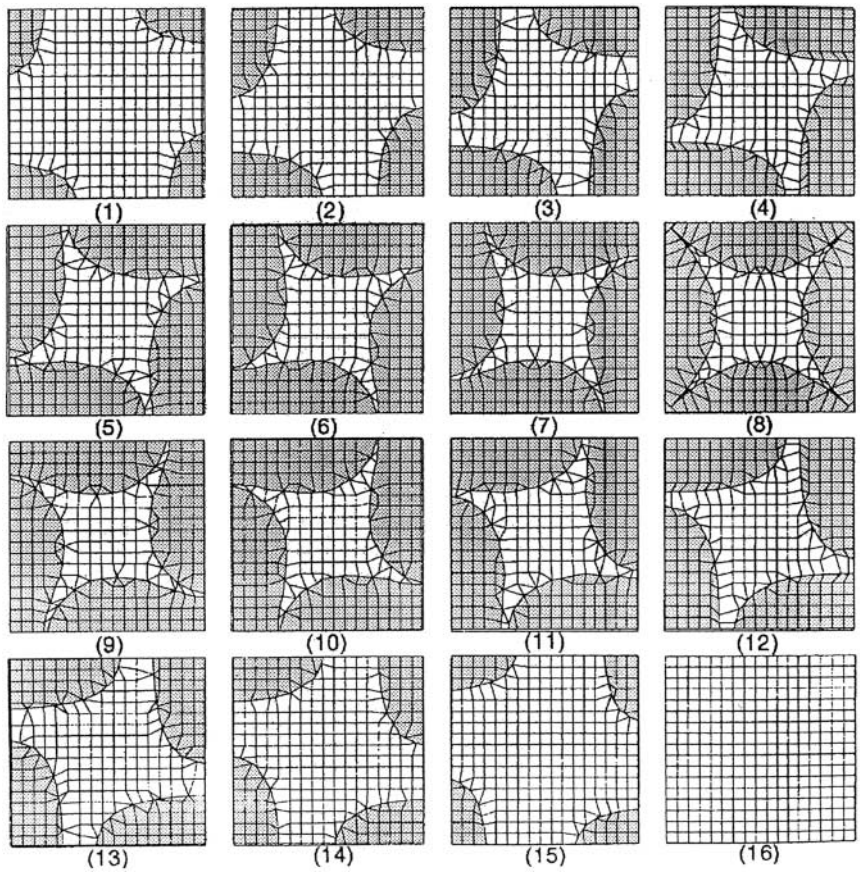

Figure 6. Top-sectional views of successive sections taken at increasing depths of $d/8$ for pore type 1 with $d = d_f = d_w$ and $l = l_f = l_w$. "▦" denotes interfiber region in multifilament fabrics.

result corresponding to each control volume is an algebraic equation containing unknown values of the dependent variable at the central grid and its immediate neighboring grids. Then the algebraic equations corresponding to all control volumes in the calculation domain are solved iteratively to obtain discrete values of the dependent variable. The sum of normalized residuals of all variables converge to less than 1×10^{-3} within 2000–3000 iterations.

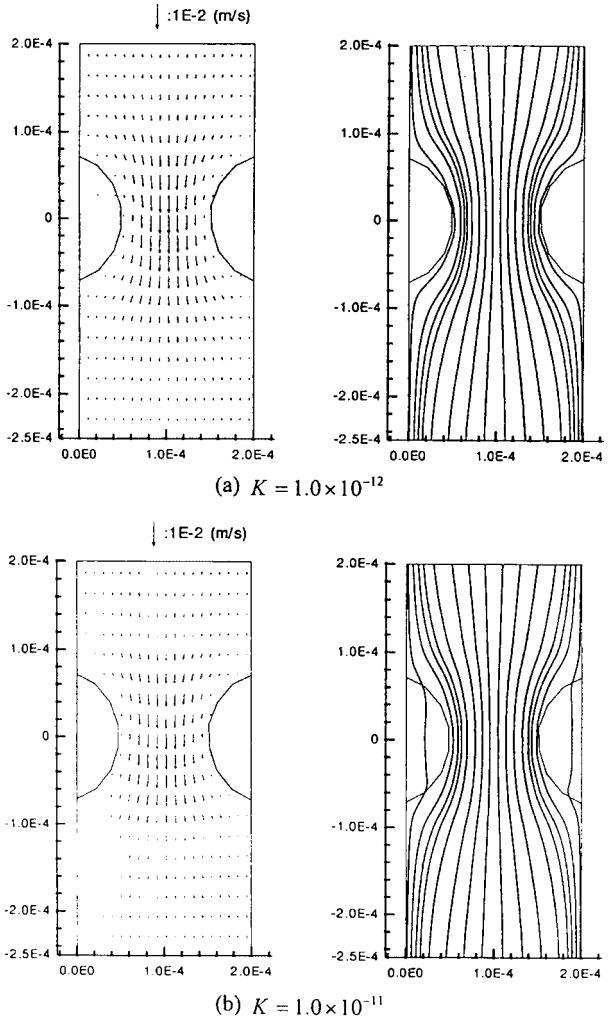

Figure 7. The velocity vectors and streamlines in the y–z plane of pore type 1 for different permeability of fabric yarn under $U_\infty = 1\times10^{-3}$ m/sec and at $x = l_f/2$.

RESULTS AND DISCUSSION

In this study, the effects of the types of fabric yarn, pore constructions, weave patterns, and upstream velocity conditions on flow pattern in multifilament fabric pore and flow resistance of multifilament filter cloth were examined.

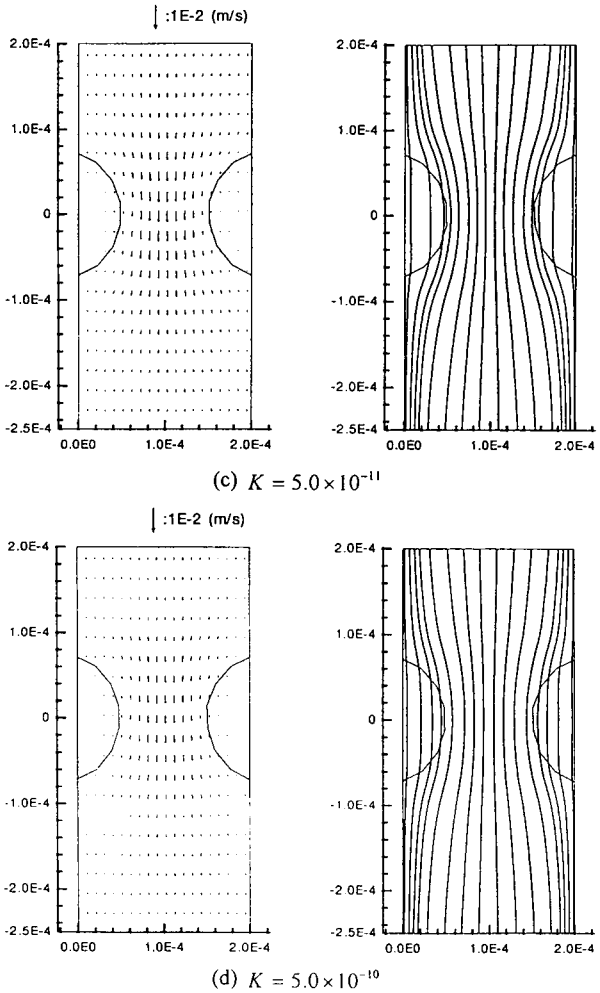

Figure 7. Continued.

Flow Pattern in Multifilament Fabric Pores

In order to describe the specific permeability of a multifilament woven filter cloth, it is necessary to determine the distribution of fluid flow between the interyarn pores, i.e., flow between the yarns of the cloth and interfiber pores, i.e., flow through the yarns. Figure 7 shows the velocity vectors and streamlines of pore type 1 for different permeability of fabric yarn under $U_\infty = 1 \times 10^{-3}$ m/sec and at $x = l_f/2$.

The results shown in Fig. 7(a)–(d) indicate that as the permeability of fabric yarn decreases, i.e., tightly twisted, there is a corresponding decline in the filtrate flux through the fabric yarn under a constant operating pressure. In this study, a homogeneous permeability, K_y, of the fabric yarn is defined to represent the tightness of the fabric yarn. The distribution of fluid flow between the interyarn and interfiber is characterized by a β factor defined as follows:

$$\beta = \frac{Q_y}{Q} \equiv \frac{K_y}{K} = \frac{\text{specific permeability of yarn}}{\text{overall specific permeability of fabric pore}} \tag{11}$$

where Q and Q_y are the overall volumetric flow rate through the fabric pore and volumetric flow rate through the yarns, respectively; K and K_y are the overall permeability of fabric pore and permeability of the yarns, respectively. A larger value of β factor indicates a loosely twisted yarn or a tightly woven fabric while a smaller value of β factor indicates a tightly twisted yarn or a loosely woven fabric. Tables 1 and 2 list typical values of β factor for various flow rates through multifilament fabric pore and various pore types, respectively. The values of β factor listed in Table 1 indicate that under a specified operating pressure, increase of the permeability of fabric yarns will result in a corresponding increase of the value of β factor. That means much of the fluid will pass around the yarn as increasing of flow rate under the same operating pressure. Table 2 lists the typical values of β factor for fluid flow through various types of woven fabric pore. The sequence of the value of β factor is: pore type 4 $>$ pore type 3 $\cong$ pore type 2 $>$ pore type 1. From a two-dimensional (2D) top view, all of the four kinds of fabric pore have the same cross-

Table 1.

K_y Values	$K_y = 1.0 \times 10^{-12}$	$K_y = 1.0 \times 10^{-11}$	$K_y = 5.0 \times 10^{-11}$	$K_y = 5.0 \times 10^{-10}$
β values				
$U_\infty = 0.001$ m/sec	0.260	0.307	0.424	0.513
$U_\infty = 0.05$ m/sec	0.103	0.181	0.270	0.392

Note: Pore type 1.

Table 2.

Types of Fabric Pore	Pore Type 1	Pore Type 2	Pore Type 3	Pore Type 4
β values	0.270	0.469	0.460	0.654

Note: $K_y = 5.0 \times 10^{-11}$ and $U_\infty = 0.05$ m/sec.

sectional area. However, in a 3-D progressive horizontal sectional view as shown in Fig. 6, it is evident that the interstice with the greatest number of yarn interlacings, type 1, has the smallest minimum cross-sectional area for relatively open fabrics while the pores with no interlacings, type 4, have the largest minimum cross-sectional area. From the observation of the flow pattern and comparison of the values of β factor among various permeabilities of fabric yarns under various operating conditions, it can be concluded that in the case of tightly woven filter cloths, i.e., a larger value of β, the flow is predominant through the yarns of the cloth and it is possible to correlate flow data in terms of the diameter of the fibers in the yarn. On the other hand, however, flow will generally be directed around the yarns of a loosely woven cloth, especially if the yarns are tightly twisted, i.e., a smaller value of β, and the yarn diameter will become more important. Many practical cases of cloths woven from multifilament yarns fall between these two extremes. Figure 7 also shows that as the permeability of fabric yarn decreases, there is a corresponding decrease in the size of the minimum cross-sectional area of streamtubes downstream. The contraction of streamtubes approach a minimum cross-sectional area as the number is increased to be zero, since in such a circumstance all of the fluid passes around the yarn and the flow rate in the interstices reaches a maximum value under a specified operating condition.

Figure 8 shows the velocity vectors and streamlines of four different fabric pores under $U_\infty = 1 \times 10^{-3}$ m/sec and at $x = l_f/2$. Comparison of the flow patterns between pore type 1 and pore type 3 shows the average velocity of pore type 1 is larger than that of pore type 3 though they have the same 2D sectional geometry. It is mainly due to the woven structure of pore type 1 being more compact than that of pore type 3, thus yielding a smaller pore area for fluid flow. Further, since the 2D sectional geometry of pore type 1, pore type 3, and pore type 4 are all in symmetry, the profiles of velocity distribution of these three pore types are all in symmetry, too. In the unsymmetrical case of pore type 2, however, the symmetrical velocity profile is not observed. The velocity above the weft yarn on the right-hand side is smaller than that of the weft yarn on the left. In other words, the surface of low-lying fabrics will be fouled first in the initial stage of cake filtration. The velocity vectors and streamlines in Figs. 7 and 8 show that the highly tortuous walls of fabrics noticeably affect the flow pattern in the interstices and the streamlines downstream, and that the surface of low-lying fabrics will be fouled first in the initial stage of cake filtration.

Flow Resistance Through Multifilament Fabric Pores

The results shown in Fig. 9 indicate that as the permeability of fabric yarn decreases, i.e., tightly twisted, there is a corresponding decline in the filtrate flux under a constant operating pressure. It is mainly due to the decrease of total

MARCEL DEKKER, INC.
270 Madison Avenue, New York, New York 10016

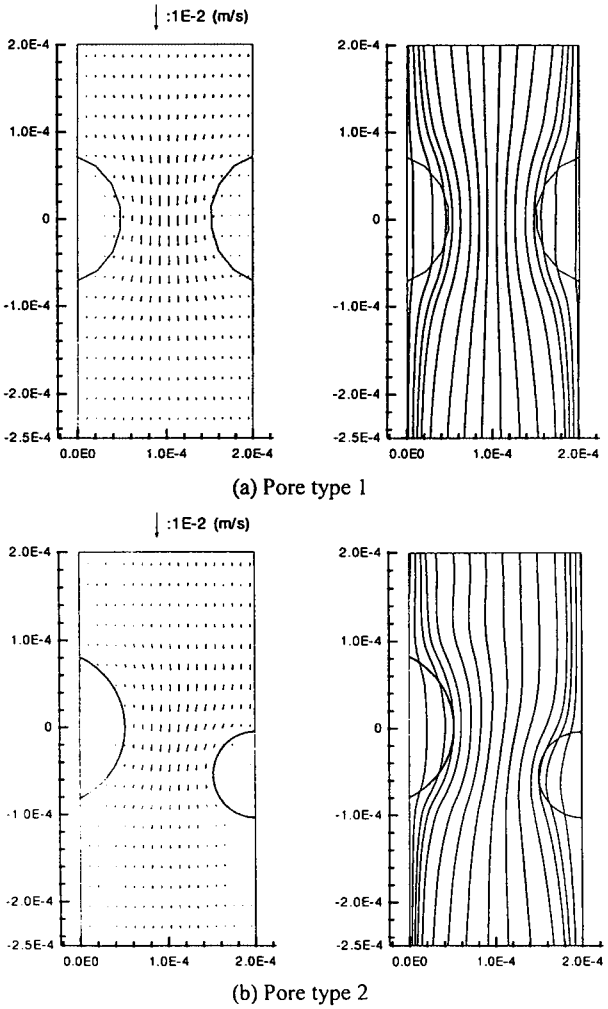

Figure 8. The velocity vectors and streamlines in the $y-z$ plane of the four different pore types under $U_\infty = 1 \times 10^{-3}\,\mathrm{m/sec}$ and $K_y = 5.0 \times 10^{-11}\,\mathrm{m}^2$ at $x = l_f/2$.

available area for fluid flow as the fabric yarn twisted tightly. Further, increasing the flow rate will result in the increase of pressure drop as well. In practice, relatively little data about flow regimes for fluid flow through filter cloths have been given in the literature for filter cloth, the major source being Heertjes' work on woven fabrics (5). Using a definition of the Reynolds number based on the pore diameter and the velocity through the pore, he reported a transition zone in

MARCEL DEKKER, INC.
270 Madison Avenue, New York, New York 10016

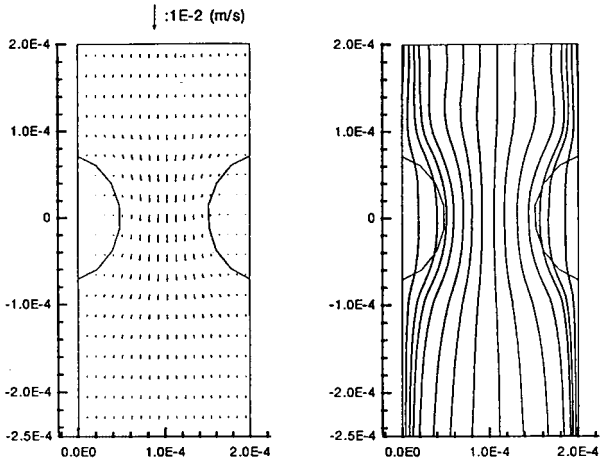

(c) Pore type 3

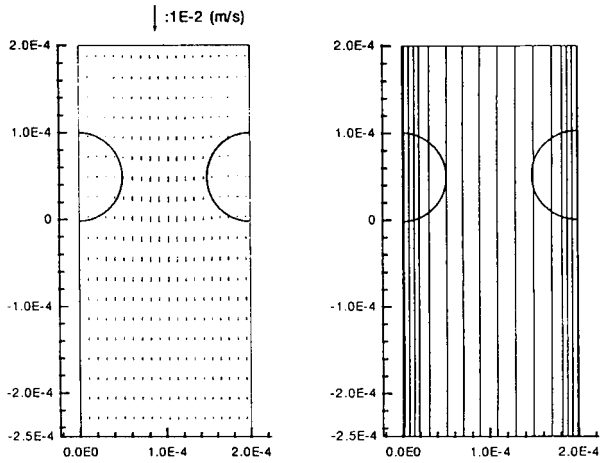

(d) Pore type 4

Figure 8. Continued.

the range $3 < Re < 7$ separating the laminar and turbulent regions. In Fig. 10, showing plots of the friction factor vs. Reynolds number, all the curves have slopes of -1 in the region $Re < 3$ (based on equivalent diameter and superficial velocity) and therefore obey the viscous flow equations. The initiation of a transition from viscous to turbulent flow with an increase in Reynolds number is seen as a change in the slope at ca. $Re = 3$.

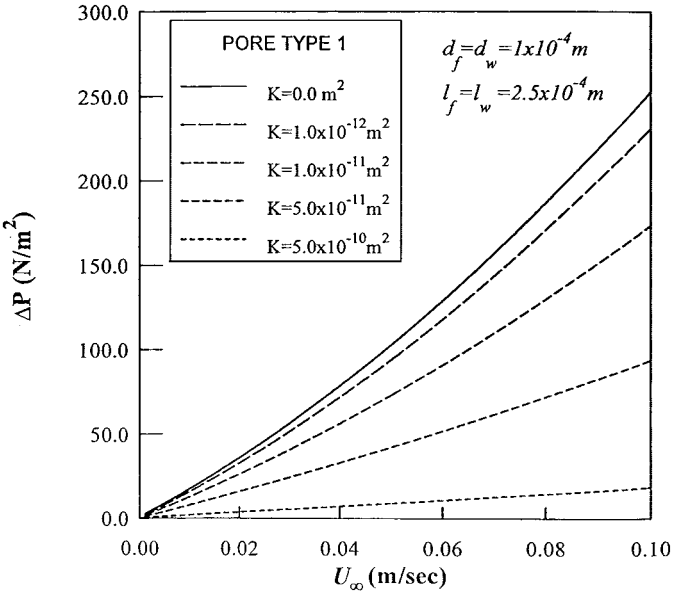

Figure 9. Pressure drop vs. superficial velocity of pore type 1 for different permeability of fabric yarn under $U_\infty = 1 \times 10^{-3}$ m/sec.

Figure 11 shows how the pressure drop of fluid flow through multifilament woven fabric will be affected by the woven structures of the fabric pore. From the progressive horizontal sections of the four fabric pore models shown by Backer (6), it is evident that the interstice with the greatest number of yarn interlacings, type 1, has the smallest minimum cross-sectional area for relatively open fabrics while the pores with no interlacings, type 4, have the largest minimum cross-sectional area. On the basis of pore-sectional area, the numerical results shown in Fig. 11 indicate that among the fabric pore models having the same yarn diameters and spacings, type 1 pores offer the highest resistance to the passage of fluid compared to the others.

Flow Resistance of Multifilament Filter Cloths

Some commercial fabric constructions have two or three types of basic unit pores beyond the plain and 2/2 twill weaves, such as the satin weave shown in Fig. 2. As shown in Fig. 1(a) and (b), the plain and 2/2 twill weaves

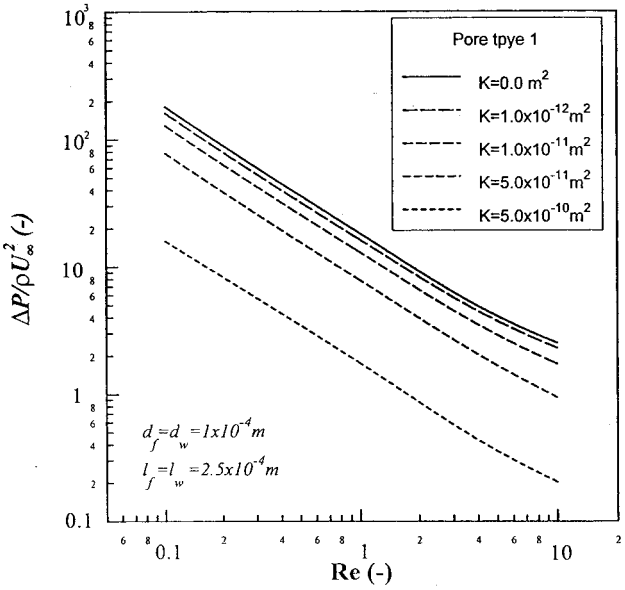

Figure 10. Dimensionless pressure drop vs. *Re* for water flow through pore type 1 for different permeability of fabric yarn under $U_\infty = 1 \times 10^{-3}$ m/sec.

consist entirely of type 1 pores and type 2 pores, respectively. The 4/1 satin, however, always contains two kinds of fabric pores, a fifth part of type 4 pores and four parts of type 2 pores, independent of their position on the fabric. Thus, under the same driving pressure, the approaching velocity, equivalent diameter, effective fraction open area, and orifice perimeter of satin weaves may be characterized by weighting the contribution of type 2 and type 4 pores through Eqs. 4(a)–(d). The results shown in Fig. 12 indicate that a multifilament fabric with plain weave will be more resistant to the passage of a fluid. Long-float 4/1 satin weaved multifilament fabric, on the other hand, with the greatest number of type 4 pores, shows the maximum permeability. This tendency is consistent with that of monofilament filter fabrics.

CONCLUSION

Fluid flow through multifilament woven filter cloths has been studied numerically by using the fluid-flow software FLUENT. The effects of types of fabric yarn and woven structures on fluid flow through the basic weaves of

MARCEL DEKKER, INC.
270 Madison Avenue, New York, New York 10016

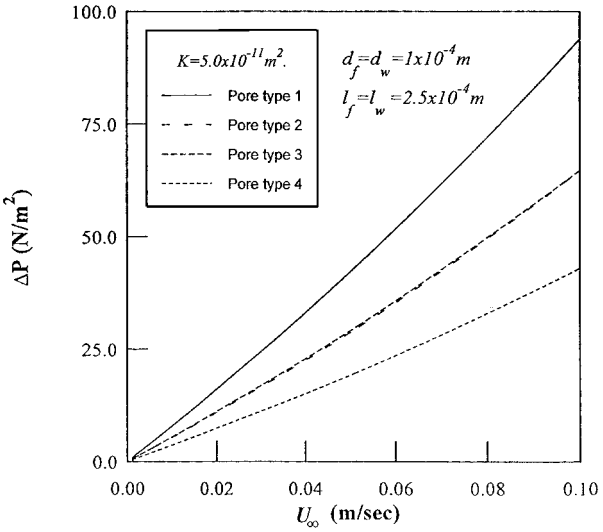

Figure 11. Pressure drop vs. superficial velocity for water flow through four different pore types under $U_\infty = 1 \times 10^{-3}$ m/sec and $K_y = 5.0 \times 10^{-11}$ m^2.

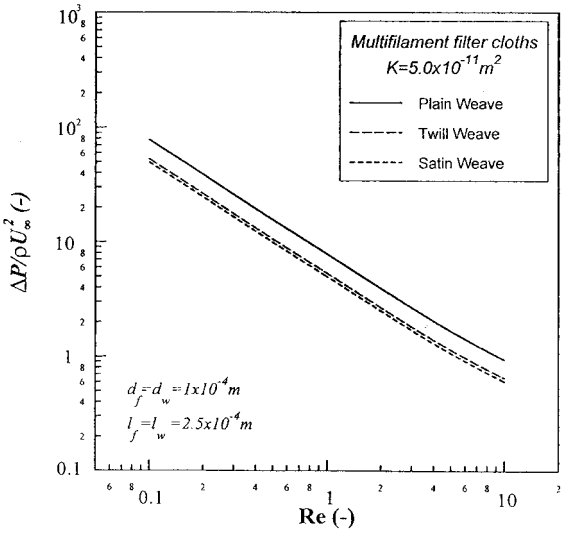

Figure 12. Dimensionless pressure drop vs. *Re* for water flow through three different weave types of multifilament filter cloth.

MARCEL DEKKER, INC.
270 Madison Avenue, New York, New York 10016

multifilament woven filter cloths were discussed. The flow pattern and the resistance to flow in the interstices were obtained as results of the numerical solution. Results of this work show that the construction of the fabric pores has a significant influence on the flow pattern in the interstices and the downstream. It is also shown that the plain weave gives the highest fluid-flow resistance while the satin weave has the lowest under the same thread count. Furthermore, in the case of tightly woven filter cloths, the flow is predominant through the yarns of the cloth; while flow will generally be directed around the yarns of a loosely woven cloth, especially if the yarns are twisted tightly.

NOMENCLATURE

A_p	area available for flow where the flow is most constricted (m^2)
C_D	discharge coefficient
C_f	weft count (1/m)
C_w	warp count (1/m)
D_o	effective orifice diameter (m)
D_e	equivalent diameter (m)
d_f	weft yarn diameter (m)
d_w	warp yarn diameter (m)
g_i	gravitational acceleration in the i direction (m\/sec^2)
g_i^*	dimensionless gravitational acceleration in the i direction
K	overall permeability of filter cloth (m^2)
K_y	permeability of the yarns (m^2)
l_f	weft yarns distance (m)
l_w	warp yarns distance (m)
P^*	dimensionless pressure
ΔP	pressure difference over filter cloth (Pa)
Q	overall volumetric flow rate through the fabric pore (m^3/sec)
Q_y	volumetric flow rate through the yarns (m^3/sec)
r_H	hydraulic radius (m)
Re	Reynolds number
U_∞	superficial velocity (m/sec)
u_p	true velocity in the fabric (m/sec)
v_j	fluid velocity in the j direction (m\/sec)
v_i^*	dimensionless velocity ($= v_i/u_\infty$) in the i direction
v_j^*	dimensionless velocity ($= v_i/u_\infty$) in the j direction
W_p	wetted perimeter of the orifice where the flow is most constricted (m)
x_i	coordinate in the i direction (m)
x_j	coordinate in the j direction (m)

MARCEL DEKKER, INC.
270 Madison Avenue, New York, New York 10016

x_i^* dimensionless coordinate ($= x_i D_e$) in the i direction
x_j^* dimensionless coordinate ($= x_j D_e$) in the j direction

Greek Letters

α_p effective fraction open area
α angle of inclination of the yarn fabric (°)
ϵ porosity
ρ fluid density (kg/m^3)
μ fluid viscosity (kg/m sec)

ACKNOWLEDGMENTS

The authors wish to express their sincere gratitude to the National Science Council of the Republic of China for its financial support.

REFERENCES

1. Rushton, A.; Griffiths, P. Fluid Flow in Monofilament Filter Media. Trans. Inst. Chem. Eng. **1971**, *49*, 49–59.
2. Bruncher, B. Caractérisation et Critères de Choix des Tissus Métalliques Filtrants. Infos. Chim. **1981**, *213*, 209–215.
3. Pedersen, G.C. Fluid Flow Through Monofilament Fabrics. Paper presented at 64th National Meeting of AIChE, New Orleans, March 1969; 16–20.
4. Robertson, A.F. Air Porosity of Open Weave Fabrics. Text. Res. J. **1950**, *20*, 838–857.
5. Heertjes, P.M. Studies in Filtration: The Initial Stages of the Cake Filtration. Chem. Eng. Sci. **1957**, *6*, 190–196.
6. Backer, S. The Relationship Between the Structural Geometry of a Textile Fabric and Its Physical Properties. Part IV: Interstice Geometry and Air Permeability. Text. Res. J. **1951**, *21*, 703–714.
7. Rushton, A.; Green, D.J.; Khoo, H.E. Flow of Fluids in Filter Cloths. Filtr. Sep. **1968**, *May/June*, 213–216.
8. McGregor, R. The Effect of Rate of Flow on Rate of Dyeing, II: The Mechanism of Fluid Flow Through Textiles and Its Significance in Dyeing. J. Soc. Dyers Colour. **1965**, *81*, 429–438.
9. van den Brekel, L.D.M.; de Jong, E.J. Hydrodynamics in Packed Textile Beds. Text. Res. J. **1989**, *59*, 433–440.
10. Rushton, A.; Green, D.J. The Analysis of Textile Filter Media. Filtr. Sep. **1968**, *Nov./Dec.*, 516–523.

MARCEL DEKKER, INC.
270 Madison Avenue, New York, New York 10016

11. Lu, W.M.; Tung, K.L.; Hwang, K.J. Fluid Flow Through Basic Weaves of Monofilament Filter Cloth. Text. Res. J. **1996**, *66* (5), 311–323.
12. Patankar, S.V. *Numerical Heat Transfer and Fluid Flow*; McGraw-Hill: New York, 1980; Chap. 6.

Received February 2001
Revised July 2001

Request Permission or Order Reprints Instantly!